Analysis of resonant detection of terahertz radiation in high-electron mobility transistor with a nanostring/carbon nanotube as mechanically floating gate

doi: 10.1063/1.2957589

Analysis of resonant detection of terahertz radiation in high-electron mobility transistor with a nanostring/carbon nanotube as the mechanically floating gate

V. G. Leiman,[1,a)] M. Ryzhii,[1] A. Satou,[1] N. Ryabova,[1] V. Ryzhii,[1] T. Otsuji,[2] and M. S. Shur[3]
[1]*Computational Nanoelectronics Laboratory, University of Aizu, Aizu-Wakamatsu 965–8580, Japan*
[2]*Research Institute for Electrical Communication, Tohoku University, Sendai 980–8577, Japan*
[3]*Department of Electrical, Computer, and Systems Engineering, Rensselaer Polytechnic Institute, Troy, New York 12180, USA*

(Received 8 April 2008; accepted 19 May 2008; published online 28 July 2008)

We develop a device model for a resonant detector of electromagnetic radiation with a frequency in the terahertz (THz) range modulated by megahertz (MHz) or gigahertz (GHz) signals based on a micromachined high-electron mobility transistor (HEMT) with a metallized nanostring (NS) or metallic carbon nanotube (CNT) as mechanically the floating gate and analyze the detector operation. The device model describes both the NS/CNT mechanical motion and plasma effects in the HEMT two-dimensional electron channel. Using this model, we calculate the output gate alternating current and the detector responsivity as functions of the carrier (in the THz range) and modulation frequencies, which are in the THz and MHz (or GHz range), respectively. It is shown that the THz detector responsivity exhibits sharp and high maxima under the conditions of both mechanical and plasma resonances. © *2008 American Institute of Physics*.
[DOI: 10.1063/1.2957589]

I. INTRODUCTION

The use of high-electron mobility transistors (HEMTs) with conducting microcantilevers (MCs) serving as mechanically floating gates can provide new functional capabilities for different device applications. The concept of such micromachined field-effect transistors was put forward and discussed a long time ago by Nathanson *et al.*[1] Micromachined HEMTs comprising MC over a two-dimensional electron gas (2DEG) channel were fabricated and characterized (see, for instance, also Refs. 2–9). If a micromachined HEMT is irradiated, the incoming radiation received by an antenna produces the alternating current (ac) voltage $\delta V(t)$ that results in the appearance of the electric field $\mathcal{E}$ between the MC and 2DEG channel. The electric force acting on MC is a nonlinear (quadratic) function of this electric field. As a result, the incoming radiation can produce the direct current (dc) force which is proportional to $\langle \mathcal{E}^2 \rangle$, where the symbol $\langle \ldots \rangle$ means the averaging over the period of the radiation ac electric field. This force affects the MC spatial position and its motion and leads to a variation of the source-drain current. When the intensity is modulated at a certain frequency much smaller than the radiation frequency, the averaged electric force acting on the MC is transient. This results in the MC mechanical oscillations with the modulation frequency and the pertinent oscillations of the displacement gate and source-drain ac's. If the modulation frequency coincides or close to the resonant frequency of the MC mechanical oscillations, the amplitude of these oscillations can be rather large. The resonant oscillations of the MC position and, hence, the oscillations of the spacing between MC and 2DEG channel, might lead to relatively large gate and source-drain ac's. Thus, micromachined HEMTs can, in principle, be used for the selective detection of modulated radiation with the modulation frequency close to the MC resonant frequency (or a half of the latter frequency). On the other hand, when the incoming radiation frequency is close to the frequencies of the plasma resonances, associated with the excitation of the self-consistent spatiotemporal variations of the electron density in the 2DEG channel and the electric field, the amplitude of the ac electric field $\mathcal{E}$ can be resonantly large. As a result, the maximum of the amplitude of the ac voltage $|\delta\varphi_\omega|$ can significantly exceed the amplitude of incoming signal δV_ω. Since the plasma resonant frequencies in HEMTs with micrometer and submicrometer characteristic sizes fall in the terahertz (THz) range, the excitation of plasma oscillations in 2DEG channels in the HEMT-like systems can be utilized in THz devices (sources, frequency multipliers, detectors, etc.) as discussed previously (see, for instance, Ref. 10). The results of experimental studies of plasma effects in HEMT-like heterostructure devices have been reported in numerous publications, in particular, in Refs. 11–21. Thus, a device based on a HEMT supplied by MC as mechanically floating gate might serve as a highly selective detector of modulated THz radiation exhibiting giant resonant response when the modulation and carrier frequencies correspond to the mechanical and plasma resonances, respectively.

The concept of such a detector of modulated THz radiation based on a micromachined HEMT and exploiting both mechanical and plasma resonances was recently considered

a)On leave from the Department of General Physics, Moscow Institute of Physics and Technology, Dolgoprudny 141700, Russia. Electronic mail: v-ryzhii@u-aizu.ac.jp.

in Refs. 22 and 23. This concept is farther evolved in this paper, where we propose and analyze a resonant detector of modulated THz radiation based on a HEMT with the mechanically floating metallized nanostring (NS) or a carbon nanotube (CNT) with metallic conductivity serving as the HEMT gate. Replacing a MC by NS or CNT and using high tensile stress, one might achieve the mechanical resonances with higher quality factor at higher frequencies. In the devices with very short gate (i.e., NS or CNT), the spectrum of the plasma oscillations in the 2DEG channel is similar to the spectrum of the waves on the surface of deep water,[10] i.e., different from the spectrum of the plasma waves in gated 2DEG channels considered previously.[22,23] The resonant excitation of mechanical oscillations of a CNT above a conducting surface by the direct effect of the ac signals was previously observed experimentally.[24] The resonant mechanical frequency was tuned by the bias voltage. The NS based systems can exhibit the quality factors exceeding 10^5 (see, for instance, Ref. 25, and references therein). Using the developed device model, we study the response of the coupled 2DEG and NS/CNT and calculate the detector responsivity as a function of the modulation and carrier frequencies and the bias voltages.

Micromechanical devices for the detection of radiation (in particular, the THz radiation) in the resonant regime were considered previously (see, for instance, Refs. 26–28). The concept proposed in Refs. 26–28 is based on the use of MCs as the resonant cavity micromirrors whose position changes under the pressure of incoming radiation. The detectors (and imaging devices on their basis) proposed and evaluated could have full optical readout and provide the circumvention of the noise limitations on the sensitivity of frequency modulation spectroscopy. In contrast to Refs. 26–28, the THz detector under consideration exploits the electrical actuation due to the interaction of the charges in the NS/CNT and 2DEG which is fairly strong. Another distinction is associated with the use of the plasma resonant cavity which is much smaller than the Fabry–Pérot resonator due to much smaller plasma wave velocity in comparison with the velocity of light. Although, the quality factor of the plasma resonators is markedly limited by the electron collisions, this disadvantage of the THz detectors with such a kind of resonators can be compensated by their small size and possible integration with other parts of the system and by direct electrical readout.

The paper is organized as follows. In Sec. II, we write down the equations governing both electron transport in the 2DEG channel and mechanical oscillations of NS/CNT coupled with an equation for the self-consistent potential. In Secs. III and IV, we derive an equation governing the averaged NS/CNT mechanical motion under the incoming modulated signals and study the NS/CNT mechanical response. Section V deals with the calculation of the signal current (the displacement current through the NS/CNT) at the modulation frequency. In Sec. VI, we calculate the responsivity of the device under consideration as a detector of modulated THz radiation using a simplified model for the detector antenna. In Sec. VII, we draw the conclusions.

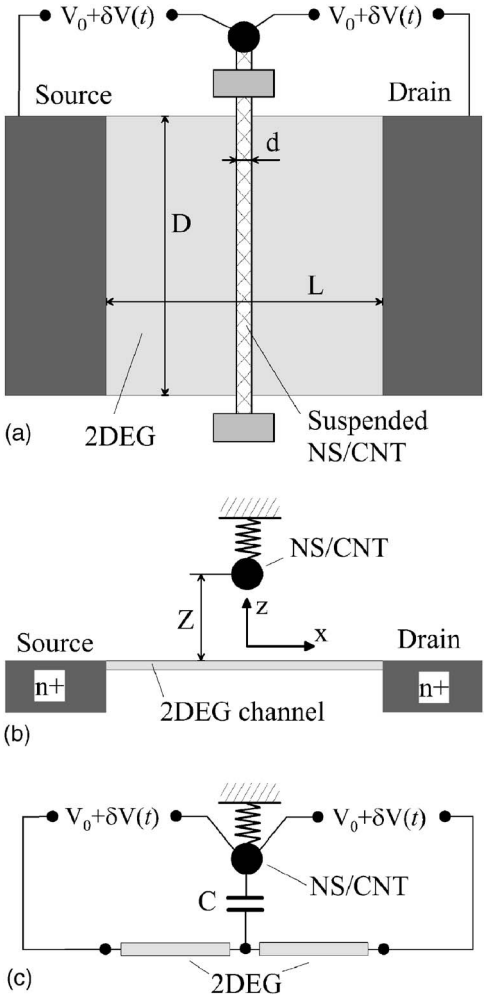

FIG. 1. Schematic view of device structure top view (a) sideview (b), and the equivalent circuit (c).

II. EQUATIONS OF THE MODEL

We consider a HEMT with a metallized NS or a metallic CNT as the HEMT mechanically floating gate. The device structure is shown schematically in Fig. 1. The axis x and the axis z are directed in the 2DEG channel plane and perpendicular to the latter, respectively. The axis y is directed along the NS/CNT. The coordinates of the NS/CNT in the absence of the applied voltages are $x=0$ and $z=W$. The electron hydrodynamic velocity, $u=u(t,x)$, along the 2DEG channel and the electron sheet density, $\Sigma=\Sigma(t,x)$, in the channel are governed by the continuity equation and Euler equation[10,22] (see also Refs. 29–33),

$$\frac{\partial \Sigma}{\partial t}+\frac{\partial \Sigma u}{\partial x}=0, \tag{1}$$

$$\frac{\partial u}{\partial t}+u\frac{\partial u}{\partial x}+\gamma u=\frac{e}{m}\left.\frac{\partial \psi}{\partial x}\right|_{z=0}. \tag{2}$$

Here, $\psi=\psi(t,x,z)$ is the electric potential, so that $\psi(t,x,z)|_{z=0}$ is the potential in the channel, $e=|e|$ and m are the electron charge and effective mass, respectively, and $\gamma=e/m\mu$ is the frequency of electron scattering with impurities, where μ is the electron mobility. The axis x is directed

in the 2DEG channel plane (perpendicular to NS/CNT), the axis y is directed along NS/CNT, and the axis z is normal to both the 2DEG channel and NS/CNT. The electric potential obeys the two-dimensional Poisson equation which in the case under consideration can be presented in the following form:

$$\frac{\partial^2 \psi}{\partial x^2} + \frac{\partial^2 \psi}{\partial z^2} = \frac{4\pi e^2(\Sigma - \Sigma_d)}{m\text{æ}} \cdot \delta(z). \tag{3}$$

The right-hand side of Eq. (3) constitutes the charge in the 2DEG channel associated with the deviation of the electron density Σ and the donor density Σ_d (immediately in the 2DEG channel or separated from it by a thin spacer). The quantity æ is the effective dielectric constant, which accounts for the difference between the dielectric constant above the channel ($\text{æ}_a \simeq 1$) and the dielectric constant of a semiconductor material below the channel ($\text{æ}_s \gg 1$). Equation (3) should be solved considering that the potentials of the source and drain contacts are $\psi=0$, while the potential of the voltage $V=V_0+\delta V(t)$ is applied to the NS/CNT. Here, $V_0<0$ is the dc bias voltage and $\delta V(t)$ is the ac component associated with the ac signal received by an antenna connected with the source and drain from one side and the NS/CNT from the other. The signal ac voltage corresponds to the carrier frequency ω (in the THz range) and the modulation frequency ω (in the range of the frequencies of the NS/CNT mechanical oscillations, say, in the gigahertz range): $\delta V(t)=\delta V_\omega[1+\alpha_m \cos \omega_m t]\cos \omega t$, where δV_ω and α_m are the amplitude and modulation depth of the signal.

The NS/CNT mechanical movement in vertical direction (perpendicular to the 2DEG plane) associated with the NS/CNT bending is described using the so-called point-mass model,[4] i.e., the consideration of the elastic NS/CNT is replaced by the consideration of a point mass M [see Fig. 1(b)] The resonant frequency of the NS/CNT oscillations, associated solely with its mechanical properties, is given by $\Omega_0 \propto 1/\sqrt{M}$, where M is the NS/CNT mass. In this model, the displacement of the NS/CNT is governed by the following equation:

$$\frac{\partial^2 Z}{\partial t^2} + \gamma_m \frac{\partial Z}{\partial t} + \Omega_0^2 (Z - W) = \frac{F}{M}, \tag{4}$$

where γ_m is the parameter characterizing the damping of the mechanical NS/CNT oscillations associated with different mechanisms of the energy loss in the NS/CNT body and in the clamps and $F=F(t)$ is the force on the NS/CNT due to the dc and ac electric fields created by the bias and signal voltages. This force accounts for the existence of the plasma oscillations in the 2DEG channel, i.e., spatiotemporal variations of the distributed electron charge in this channel.

When the spacing between the source and drain contacts $L \gg W$, the displacement current between the 2DEG and NS/CNT is located in fairly small region (with the size about W) near the point $x=0$. In this case, one can use a simplified approach in which a narrow region under the NS/CNT is replaced by an equivalent circuit [comprising a capacitor connected with the center of the 2DEG channel as shown in Fig. 1(c)]. For the NS/CNT capacitance we use the following approximate expression: $C=D/2\ln(4Z/d)$, where D is the NS/CNT length, d is its diameter (characteristic transverse size) and Z is the spacing between the NS/CNT and 2DEG channel.

III. EQUATION FOR THE AVERAGED NS/CNT MOTION

The term on the right-hand side of Eq. (4) represents the electric force acting on NS/CNT associated with the bias and ac voltages. In the framework of our model, this force can be expressed via the potential drop between the NS/CNT and the center of the channel (see, for instance, Ref. 9),

$$F = -\frac{1}{2}\frac{\partial C}{\partial Z}(V - \varphi|_{x=0})^2, \tag{5}$$

where $\varphi=\psi|_{z=0}$. Due to fairly large difference in the carrier frequency, ω, of the incoming THz radiation, on the one hand, and the modulation frequency, ω_m (and, hence, the characteristic frequency of the NS/CNT mechanical oscillations Ω_0), on the other, the NS/CNT motion is actually determined by the force $\langle F \rangle$ which is the quantity $F=F(t)$ averaged over high-frequency, i.e., THz oscillations. Here, and in the following, the symbol $\langle \ldots \rangle$ denotes the averaging over the period $\tau=2\pi/\omega$.

As in Refs. 22 and 23, considering that $\omega_m, \Omega_0 \ll \omega$, the solutions of the earlier equations are searched in the form $\varphi=\langle\varphi\rangle+\delta\varphi_\omega$, $\Sigma=\langle\Sigma\rangle+\delta\Sigma_\omega$, and $Z=\langle Z\rangle+\delta Z_\omega$. Here, the averaged components are assumed to be slowly varying with time (with the frequency of the order of ω_m), and $\delta\varphi_\omega$, $\delta\Sigma_\omega$, and δZ_ω are the pertinent small components strongly oscillating with the frequency ω. In this case, the ac potential distribution along the channel $\varphi_\omega=\psi_\omega|_{z=0}$ can be found neglecting slow variations of Z and be searched in the following form:

$$\delta\varphi_\omega = A \sin[q_\omega(x - L/2)], \quad (x > 0), \tag{6}$$

$$\delta\varphi_\omega = A \sin[q_\omega(x + L/2)], \quad (x < 0). \tag{7}$$

Here,

$$q_\omega = \frac{\text{æ} m\omega(\omega + i\gamma)}{2\pi e^2 \Sigma_d}. \tag{8}$$

Taking into account that the electron current along the 2DEG channel near its center (at the points $x=+0$ and $x=-0$) can be presented as

$$\delta J_\omega = -D\sigma_\omega \left.\frac{d\varphi_\omega}{dx}\right|_{x=\pm 0}, \tag{9}$$

where

$$\sigma_\omega = i\frac{e^2\Sigma_d}{m(\omega + i\gamma)} \tag{10}$$

is the 2DEG ac conductivity, and equalizing $2\delta J_\omega$ and the displacement current, $\delta J\omega^g$, between the 2DEG and NS/CNT(gate current)

$$\delta J^g_\omega = -i\omega C(\delta V_\omega - \delta\varphi_\omega|_{x=0}), \tag{11}$$

we obtain

$$\delta\varphi_\omega|_{x=0} = \delta V_\omega \frac{c}{[c - \cot(q_\omega L/2)]}, \tag{12}$$

where $c = \pi C/æD$.

Using Eq. (12) and averaging the left-hand and right-hand sides of Eq. (4) over high-frequency oscillations, we arrive at the following equation:

$$\frac{\partial^2\langle Z\rangle}{\partial t^2} + \gamma_m\frac{\partial\langle Z\rangle}{\partial t} + \Omega_0^2(\langle Z\rangle - W) = \frac{\langle F\rangle}{M}, \tag{13}$$

where

$$\langle F\rangle = -\frac{1}{2}\left.\frac{\partial C}{\partial Z}\right|_{Z=\langle Z\rangle}\{V_0^2 + |\delta\varphi_\omega|^2\langle\cos^2\omega t\rangle[1 + \alpha_m\cos\omega_m t]^2\}. \tag{14}$$

After that, invoking Eq. (12), we present Eq. (13) in the following form:

$$\frac{\partial^2\langle Z\rangle}{\partial t^2} + \gamma_m\frac{\partial\langle Z\rangle}{\partial t} + \Omega_m^2(\langle Z\rangle - Z_0) = \frac{1}{4M}\left.\frac{\partial C}{\partial Z}\right|_{Z=\langle Z\rangle}\mathcal{F}_\omega|\delta V_\omega|^2[1 + \alpha_m\cos\omega_m t]^2. \tag{15}$$

Here,

$$\Omega_m^2 = \Omega_0^2 - \frac{V_0^2}{2M}\left.\frac{\partial^2 C}{\partial Z^2}\right|_{Z=Z_0} \tag{16}$$

is the MC mechanical resonant frequency modified by the dc bias voltage. The dc position of the NS/CNT under the effect of the dc bias voltage is given by the following equation:

$$Z_0 - W = \frac{V_0^2}{2M\Omega_0^2}\left.\frac{\partial C}{\partial Z}\right|_{Z=Z_0}. \tag{17}$$

The factor associated with the plasma resonant response (the plasma response function) is given by

$$\mathcal{F}_\omega = \frac{c^2}{\left[c + \dfrac{\sin(\pi\omega^2/\Omega^2)}{\cos(\pi\omega^2/\Omega^2) - \cosh(\pi\gamma\omega/\Omega^2)}\right]^2 + \left[\dfrac{\sinh(\pi\gamma\omega/\Omega^2)}{\cos(\pi\omega^2/\Omega^2) - \cosh(\pi\gamma\omega/\Omega^2)}\right]^2}. \tag{18}$$

Here, we have introduced the characteristic (fundamental) plasma frequency

$$\Omega = \sqrt{\frac{2\pi^2 e^2\Sigma_d}{mæL}}. \tag{19}$$

For the 2DEG with sufficiently high electron mobility, in which $\gamma \ll \Omega$, Eq. (18) yields

$$\mathcal{F}_\omega = \frac{c^2}{\left[c + \dfrac{\sin(\pi\omega^2/\Omega^2)}{\cos(\pi\omega^2/\Omega^2) - 1}\right]^2 + \left[\dfrac{(\pi\gamma\omega/\Omega^2)}{\cos(\pi\omega^2/\Omega^2) - 1}\right]^2}, \tag{20}$$

and the resonant plasma frequency can be determined from the following equation:

$$\frac{\sin(\pi\omega^2/\Omega^2)}{1 - \cos(\pi\omega^2/\Omega^2)} = c. \tag{21}$$

At small values of c, the resonant plasma frequencies are given by

$$\omega \simeq \sqrt{(2n-1)}\left[1 - \frac{c}{\pi(2n-1)}\right]\Omega, \tag{22}$$

where $n = 1, 2, 3, \ldots$ is the plasma mode index. The frequency of the fundamental plasma mode $(n=1)$ is equal to $\Omega_p = (1 - c/\pi)\Omega$. The maximum value of $\mathcal{F}_\omega$ at the nth plasma resonance is given by

$$\max\mathcal{F}_\omega \simeq \frac{4c^2}{\pi^2(2n-1)}\left(\frac{\Omega}{\nu}\right)^2 = \frac{4C^2}{æ^2D^2(2n-1)}\left(\frac{\Omega}{\gamma}\right)^2 = \frac{1}{\ln^2(4Z_0/d)æ^2(2n-1)}\left(\frac{\Omega}{\gamma}\right)^2. \tag{23}$$

The plasma response function $\mathcal{F}_\omega$ calculated using Eq. (20) for different values of the plasma resonance quality factor $Q = \Omega/\gamma$ is shown in Fig. 2. As seen from Fig. 2, $\mathcal{F}_\omega$ exhibits sharp peaks at $\omega/\Omega \lesssim 1, \sqrt{3}, \sqrt{5}, \ldots$. The heights of the peaks increase with increasing quality factor and decrease with increasing peak index according to Eq. (23).

IV. NS/CNT MECHANICAL OSCILLATIONS

Using Eq. (15), one can find the variation of the NS/CNT position at the modulation frequency ω_m and its har-

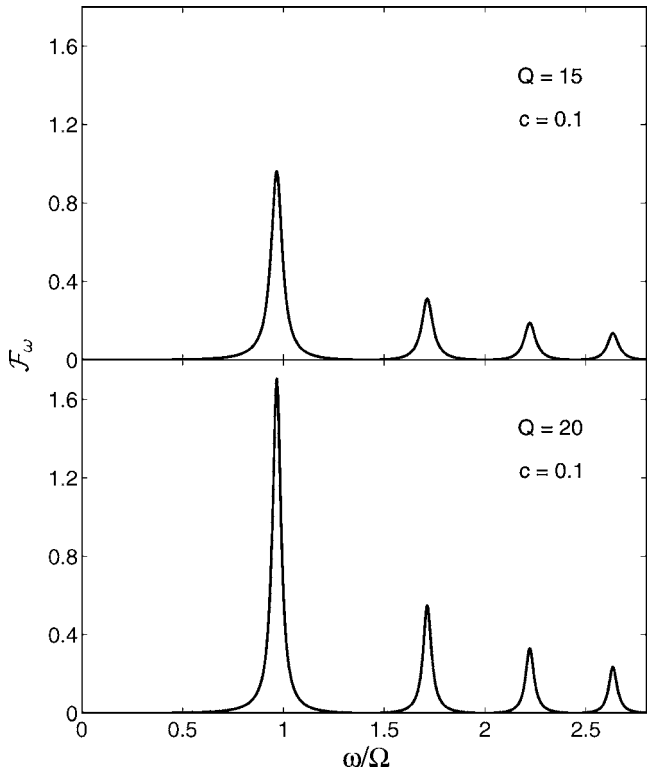

FIG. 2. The plasma response function for different values of plasma resonance quality factor ($Q=15$ and 20).

monics. Assuming that the intensity of the incoming THz radiation is sufficiently weak, so that the NS/CNT exhibits linear oscillations, for the case of moderate modulation (the modulation depth $\alpha_m<1$, and the terms proportional to α_m^2 can be omitted) we obtain

$$\langle Z\rangle - Z_0 = \frac{1}{4M\Omega_m^2}\left.\frac{\partial C}{\partial Z}\right|_{Z=Z_0}\left[1+2\alpha_m\frac{\Omega_m^2\cos(\omega_m t+\theta_m)}{\sqrt{(\omega_m^2-\Omega_m^2)^2+\gamma_m^2\omega_m^2}}\right]\times\mathcal{F}_\omega|\delta V_\omega|^2, \tag{24}$$

where θ_m is the phase shift. Near the combined resonance ($\omega_m\sim\Omega_m$ and $\omega\sim\Omega_p$) for the amplitude of the NS/CNT mechanical oscillations with the frequency ω_m, Eq. (24) yields

$$\frac{\Delta\langle Z\rangle}{W}\simeq\frac{2\alpha_m}{\pi^2\text{æ}^{*2}\Lambda^2}\frac{\Omega_m^2}{\sqrt{(\omega_m^2-\Omega_m^2)^2+\gamma_m^2\omega_m^2}}\frac{\Omega^2}{[4(\omega-\Omega)^2+\gamma^2]}\times\left(\frac{\delta V_\omega}{\bar{V}_0}\right)^2, \tag{25}$$

where

$$\bar{V}_0=\sqrt{(M\Omega_m^2W^2/D)} \tag{26}$$

is the characteristic voltage and $\Lambda=\ln(4W/d)$.

At the combined resonance ($\omega_m=\Omega_m$ and $\omega=\Omega_m\simeq\Omega$), the quantity $\Delta\langle Z\rangle$ exhibits a maximum

$$\max\frac{\Delta\langle Z\rangle}{W}=\frac{2\alpha_m Q_m Q^2}{\pi^2\text{æ}^{*2}}\left(\frac{\delta V_\omega}{\bar{V}_0}\right)^2, \tag{27}$$

where $Q_m=\Omega_m/\gamma_m\gg1$ and $Q=\Omega/\gamma\gg1$ are the quality factors of the mechanical and plasma resonances, respectively. If the carrier frequency ω is markedly smaller than the fundamental resonant plasma frequency Ω_p, instead of Eq. (27) we obtain

$$\max\frac{\Delta\langle Z\rangle}{W}=\frac{\alpha_m Q_m}{2\pi^2\text{æ}^{*2}}\left(\frac{\delta V_\omega}{\bar{V}_0}\right)^2. \tag{28}$$

V. OUTPUT SIGNAL CURRENT

The mechanical oscillations of the NS/CNT result in the periodical variations (with the modulation frequency ω_m) of the NS/CNT capacitance. As a result, the displacement current with the amplitude $\Delta J_g^{(\omega_m)}$ and the frequency ω_m through the NS/CNT (gate current) occurs

$$\Delta J_g^{(\omega_m)}=\omega_m V_0\left.\frac{\partial C}{\partial Z}\right|_{Z=\langle Z\rangle}\Delta\langle Z\rangle. \tag{29}$$

Using Eqs. (25) and (29), we obtain

$$\Delta J_g^{(\omega_m)}=\frac{DV_0}{\pi^2\text{æ}^{*2}\Lambda^4}\frac{\alpha_m\omega_m\Omega_m^2}{\sqrt{(\omega_m^2-\Omega_m^2)^2+\gamma_m^2\omega_m^2}}\frac{\Omega^2}{[4(\omega-\Omega)^2+\gamma^2]}\times\left(\frac{\delta V_\omega}{\bar{V}_0}\right)^2, \tag{30}$$

One can see that the signal current is proportional to the modulation depth of the incoming THz radiation. It is interesting that the right-hand side of Eq. (30) comprises two factors which can be fairly large, when the modulation and carrier frequencies approach to their resonant values.

VI. DETECTOR RESPONSIVITY

The detector responsivity can be defined as $\mathcal{R}_\omega^{(\omega_m)}=\Delta J_g^{(\omega_m)}/P_\omega$, where P_ω is the THz power incoming to the detector antenna. The quantities P_ω and $(\delta V_\omega)^2$ are related to each other as[10]

$$P_\omega=\frac{c_l G}{2\pi^2}(\delta V_\omega)^2, \tag{31}$$

where c_l is the speed of light and G is the antenna gain, which is approximately equal to 1.5 for the dipole antenna. From Eqs. (30) and (31), we obtain

$$\mathcal{R}_\omega^{(\omega_m)}=\frac{bDV_0}{c_l\bar{V}_0^2}\frac{\alpha_m\omega_m\Omega_m^2}{\sqrt{(\omega_m^2-\Omega_m^2)^2+\gamma_m^2\omega_m^2}}\frac{\Omega^2}{[4(\omega-\Omega)^2+\gamma^2]}, \tag{32}$$

where $b=2/(G\text{æ}^2\Lambda^4)\ll1$. Figures 3 and 4 show the detector responsivity versus the normalized carrier and modulation frequencies, ω/Ω and ω_m/Ω_m, calculated using Eq. (32) for different (rather small) values of the quality factors of plasma and mechanical resonances, $Q=\Omega/\gamma$ $Q_m=\Omega_m/\gamma_m$.

Using Eq. (32), for the detector responsivity at the combined resonance, where the responsivity reaches a maximum, we obtain

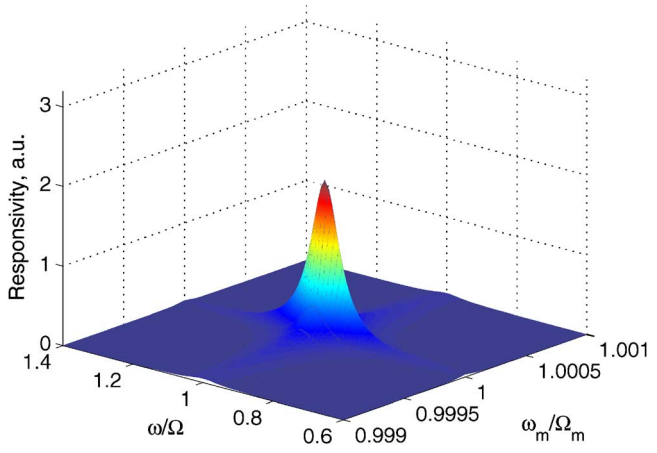

FIG. 3. (Color online) Responsivity as a function of carrier and modulation frequencies: $Q_m=2\times10^4$ and $Q=10$.

$$\max \mathcal{R}_{\omega}^{(\omega_m)} = bDV_0\frac{\alpha_m\Omega_m Q_m Q^2}{c_l\bar{V}_0^2} \propto (D/M)(V_0\Omega^2/\gamma_m\gamma^2), \tag{33}$$

Considering a HEMT with a NS similar to that fabricated and measured in Ref. 25 and assuming $\varpi=6$, $W=200$ nm, $d=150$ nm, and $G=1.5$, one obtains $b\simeq5\times10^{-3}$. The smallness of the factor b is associated with a small NS/CNT capacitance and relatively large dielectric constant of the substrate. For the device under consideration with a NS made of a material with the density 2.7 g/cm^3, $\Omega_m/2\pi=30$ MHz, and the earlier values of other parameters, we obtain $\bar{V}_0\simeq1.6$ V. Assuming that $D=15$ μm and $V_0=1.6$ V (i.e., $V_0=\bar{V}_0$), we obtain max $\mathcal{R}_{\omega}^{(\omega_m)}\simeq3\times10^{-8}\alpha_m Q_m Q^2$ A/W. If $Q_m=4\times10^4$,[25] $Q=20$, and $\alpha_m=1$, we obtain max $\mathcal{R}_{\omega}^{(\omega_m)}\simeq0.48$ A/W.

If $\varpi=6$, $m=6\times10^{-29}$ g, $\Sigma_d=10^{12}$ cm^{-2}, and $L=3.2$ μm, the fundamental plasma frequency is equal to $\Omega/2\pi=1$ THz. In this case, the quality factor $Q=20$, as in the earlier estimate, corresponds to the electron mobility $\mu=8\times10^4$ cm^2/V s, which can be achieved at liquid nitrogen or lower temperatures. At room temperature, setting (say, for a device with a GaAs channel) $\mu=1\times10^4$ cm^2/V s, one obtains max $\mathcal{R}_{\omega}^{(\omega_m)}\simeq7.5\times10^{-3}$ A/W. However, in the case of higher plasma frequency (and hence, higher carrier frequency of the detected THz radiation), the room temperature responsivity can be markedly larger than in the latter estimate. Indeed, setting $\Omega/2\pi=4$ THz, we obtain $Q=10$ and, consequently, max $\mathcal{R}_{\omega}^{(\omega_m)}\simeq0.12$ A/W.

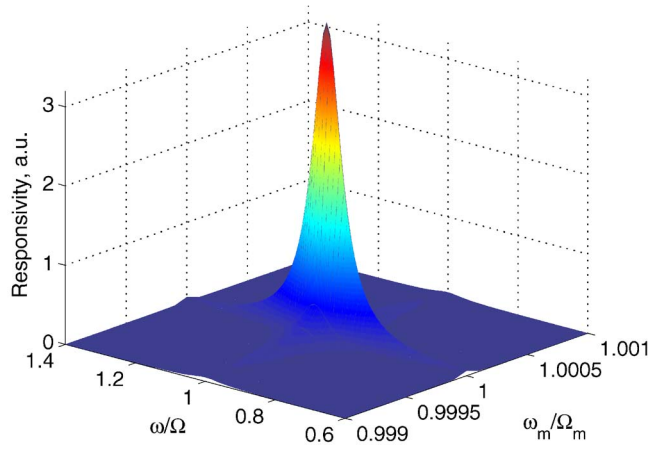

FIG. 4. (Color online) The same as in Fig. 2 but for $Q_m=4\times10^4$, $Q=10$.

One needs to note that the dc bias voltage V_0 should be smaller than the so-called pull-in voltage $\tilde{V}_0$. Analysis of Eq. (17) results in the following estimate for the pull-in voltage:

$$\tilde{V}_0 \simeq \frac{\overline{V_0\Lambda}}{\sqrt{2}}. \tag{34}$$

For the device parameters used earlier, $\tilde{V}_0/\overline{V_0}\gtrsim1$.

VII. CONCLUSIONS

We developed a device model for a resonant detector of modulated THz radiation based on a micromachined HEMT with a NS or metallic CNT as mechanically floating gate and evaluated the device performance. It was demonstrated that the output gate ac current at the modulation frequency and the detector responsivity as functions of the carrier and modulation frequencies exhibit sharp resonant peak(s) when these frequencies coincide with the frequencies of the plasma and mechanical resonances. The estimates show that the device under consideration can serve as a highly selective detector of modulated THz radiation with fairly large responsivity provided sufficiently large quality factors of the plasma and mechanical resonances. The main competitors of the micromachined resonant THz detector exploiting the nonlinearity of the force acting on MS/CNT considered earlier are the detectors also utilizing plasma resonances but other mechanisms of nonlinearity. These are the HEMT-like detectors using the mechanisms which can be attributed to the nonlinearity of the electron transport in the channel, i.e., the so-called hydrodynamic nonlinearity[10] (see also Refs. 12 and 34–36), the heating or bolometric nonlinearity,[11,20,37] the nonlinearity of the voltage dependence of the current from the channel to the gate (i.e., leakage current),[38] and the current through the electrically induced barriers in the channel[21,37] or the Schottky drain (or source) contact.[39] The strength of such nonlinearity mechanisms can be smaller and higher than that of the electromechanical mechanism depending on the device optimization. However, the use of the combined plasma and mechanical resonances can provide effective selectivity and better noise performance owing to frequency filtering (see, for instance, Ref. 26).

We considered the device with a single NS/CNT [as shown in Fig. 1(a)] which exhibits the resonant response at the modulation frequency $\omega_m=\Omega_m$ [or at $\omega_m=\Omega_m/2$, as follows from Eq. (15)]. In the HEMT-like structures with several parallel NSs/CNTs pulled over the 2DEG channel (shown schematically in Fig. 5) and characterized by different mechanical resonant frequencies Ω_m^k, where $k=1,2,3,\ldots$ is the NS/CNT index (NS or CNT "guitar"), the detection of THz radiation modulated at several definite frequencies can be possible. Due to stronger coupling of the NS/CNT array with the plasma oscillations, the NS or CNT guitar can exhibit higher responsivity at each mechanical resonant frequency Ω_m^k.

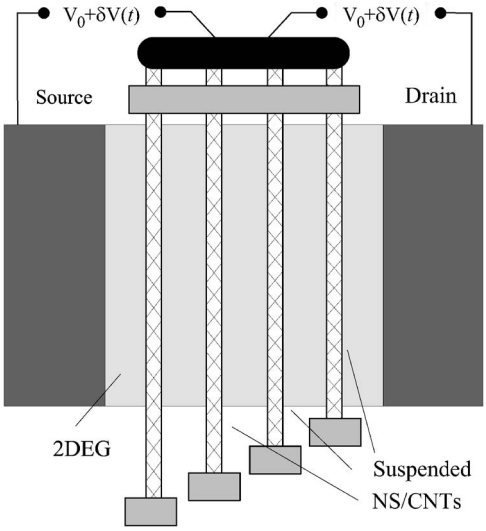

FIG. 5. Schematic view of device structure with a NS/CNT array (top view).

ACKNOWLEDGMENTS

This work was partially supported by the Grant-in-Aid for Scientific Research (S) from the Japan Society for Promotion of Science, Japan.

[1]H. C. Nathanson, W. E. Newell, R. A. Wickstrom, and J. R. Davis, Jr., IEEE Trans. Electron Devices **14**, 117 (1967).
[2]W. H. Teh, R. Crook, C. G. Smith, H. E. Beere, and D. A. Ritchie, J. Appl. Phys. **97**, 114507 (2005).
[3]R. G. Beck, M. A. Eriksson, R. A. Westervelt, K. L. Campman, and A. C. Gossard, Appl. Phys. Lett. **68**, 3763 (1996).
[4]U. Rabe, K. Janser, and W. Arnold, Rev. Sci. Instrum. **67**, 3281 (1996).
[5]M. P. Schwarz, D. Grundler, I. Meinel, Ch. Heyn, and D. Heitmann, Appl. Phys. Lett. **76**, 3564 (2000).
[6]H. Yamaguchi, S. Miyashita, and Y. Hirayama, Appl. Phys. Lett. **82**, 394 (2003).
[7]K. L. Ekunchi and M. L. Roukes, Rev. Sci. Instrum. **76**, 161101 (2005).
[8]Y. Tsuchiya, K. Takai, N. Momo, T. Nagami, H. Mizuta, S. Oda, S. Yamaguchi, and T. Shimada, J. Appl. Phys. **100**, 094306 (2006).
[9]R. C. Batra, M. Porfiri, and D. Spinello, J. Microelectromech. Syst. **15**, 1175 (2006).
[10]M. Dyakonov and M. Shur, IEEE Trans. Electron Devices **43**, 1640 (1996).
[11]X. G. Peralta, S. J. Allen, M. C. Wanke, N. E. Harff, J. A. Simmons, M. P. Lilly, J. L. Reno, P. J. Burke, and J. P. Eisenstein, Appl. Phys. Lett. **81**, 1627 (2002).
[12]W. Knap, Y. Deng, S. Rumyantsev, and M. S. Shur, Appl. Phys. Lett. **81**, 4637 (2002).
[13]N. Sekine, K. Hirakawa, M. Vosseburger, P. Haring Bolivar, and H. Kurz, Phys. Rev. B **64**, 201323 (2001).
[14]Y. Deng, R. Kersting, J. Xu, R. Ascazubi, X.-C. Zhang, M. S. Shur, R. Gaska, G. S. Simin, M. Asif Khan, and V. Ryzhii, Appl. Phys. Lett. **84**, 70 (2004).
[15]W. Knap, J. Lusakowski, T. Parently, S. Bollaert, A. Cappy, V. V. Popov, and M. S. Shur, Appl. Phys. Lett. **84**, 2331 (2004).
[16]J. Lusakowski, W. Knap, N. Dyakonova, L. Varani, J. Mateos, T. Gonzales, Y. Roelens, S. Bullaert, A. Cappy, and K. Karpierz, J. Appl. Phys. **97**, 064307 (2005).
[17]F. Teppe, D. Veskler, V. Yu. Kachorovskii, A. P. Dmitriev, X. Xie, X.-C. Zhang, S. Rumyantsev, W. Knap, and M. S. Shur, Appl. Phys. Lett. **87**, 022102 (2005).
[18]T. Otsuji, M. Hanabe, and O. Ogawara, Appl. Phys. Lett. **85**, 2119 (2004).
[19]M. Hanabe, T. Otsuji, T. Ishibashi, T. Uno, and V. Ryzhii, Jpn. J. Appl. Phys., Part 1 **44**, 3842 (2005).
[20]E. A. Shaner, M. Lee, M. C. Wanke, A. D. Grine, J. L. Reno, and S. J. Allen, Appl. Phys. Lett. **87**, 193507 (2005).
[21]E. A. Shaner, M. Lee, M. C. Wanke, A. D. Grine, J. L. Reno, and S. J. Allen, IEEE Photonics Technol. Lett. **18**, 1925 (2006).
[22]V. Ryzhii, M. Ryzhii, Y. Hu, I. Hagiwara, and M. S. Shur, Appl. Phys. Lett. **90**, 203503 (2007).
[23]Y. Hu, M. Ryzhii, I. Hagiwara, M. S. Shur, and V. Ryzhii, Phys. Status Solidi C **5**, 277 (2008).
[24]V. Sazonova, Y. Yaish, H. Ustunel, S. Tiwari, and P. L. McEuen, Nature (London) **431**, 284 (2004).
[25]S. S. Verbridge, J. M. Parpia, R. B. Reichenbach, L. M. Bellan, and H. G. Craighead, J. Appl. Phys. **99**, 124304 (2006).
[26]B. M. Chernobrod, G. P. Berman, and P. W. Milonni, Appl. Phys. Lett. **85**, 3896 (2004).
[27]G. P. Berman, A. R. Bishop, B. M. Chernobrod, M. E. Hawley, and G. W. Brown, J. Phys.: Conf. Ser. **38**, 171 (2006).
[28]G. P. Berman, B. M. Chernobrod, A. R. Bishop, and V. N. Gorshkov, e-print arXiv:physics/0703042 (2007).
[29]A. P. Dmitriev, A. S. Furman, and V. Yu. Kachorovskii, Phys. Rev. B **54**, 14020 (1996).
[30]S. Rudin and G. Samsonidze, Phys. Rev. B **58**, 16369 (1998).
[31]F. J. Crowne, J. Appl. Phys. **82**, 1242 (1997).
[32]A. Satou, V. Ryzhii, I. Khmyrova, M. Ryzhii, and M. S. Shur, J. Appl. Phys. **95**, 2084 (2004).
[33]V. Ryzhii, A. Satou, W. Knap, and M. S. Shur, J. Appl. Phys. **99**, 084507 (2006).
[34]W. Knap, Y. Deng, S. Rumyantsev, J.-Q. Lu, M. S. Shur, C. A. Saylor, and L. C. Brunel, Appl. Phys. Lett. **80**, 3433 (2002).
[35]F. Teppe, W. Knap, D. Veksler, M. S. Shur, A. P. Dmitriev, V. Yu. Kachorovski, and S. Rumyantsev, Appl. Phys. Lett. **87**, 052107 (2005).
[36]J. Torres, P. Nouvel, A. Akwaoue-Ondo, L. Chusseau, F. Teppe, A. Shcherepetov, and S. Bollaert, Appl. Phys. Lett. **89**, 201101 (2006).
[37]V. Ryzhii, A. Satou, T. Otsuji, and M. S. Shur, J. Appl. Phys. **103**, 014504 (2008).
[38]A. Satou, I. Khmyrova, V. Ryzhii, and M. S. Shur, Semicond. Sci. Technol. **18**, 460 (2003).
[39]V. Ryzhii and M. S. Shur, Jpn. J. Appl. Phys., Part 2 **45**, L1118 (2006).